Optics Letters

Photonics-based multi-function analog signal processor based on a polarization division multiplexing Mach–Zehnder modulator

YAMEI ZHANG AND SHILONG PAN*

Key Laboratory of Radar Imaging and Microwave Photonics, Ministry of Education, Nanjing University of Aeronautics and Astronautics, Nanjing 210016, China
**Corresponding author: pans@ieee.org*

Received 18 August 2017; revised 4 November 2017; accepted 6 November 2017; posted 7 November 2017 (Doc. ID 304769); published 1 December 2017

A photonics-based multi-function analog signal processor based on an optical polarization division multiplexing dual-parallel Mach–Zehnder modulator is proposed and demonstrated, which can implement simultaneously photonic microwave phase shifting, upconversion/downconversion and filtering with excellent tunability. An experiment is carried out. Downconverted and upconverted phase shifters with phases continuously tuned from −180 to 180 deg over 0–11 and 11–33 GHz are implemented. Based on the frequency-mixed phase shifter, a four-tap microwave photonic filter that has the capability to select a frequency-mixed component is built. The proposed approach features multi-function, scalable independent channels, a wide bandwidth, and high tunability, which can find applications in beamforming networks, radio frequency frontends, and radio over fiber systems. © 2017 Optical Society of America

OCIS codes: (050.5080) Phase shift; (060.5625) Radio frequency photonics; (070.1170) Analog optical signal processing.

https://doi.org/10.1364/OL.42.005034

Microwave signal processors, such as microwave phase shifters, upconverters/downconverters and filters, are commonly used in analog systems. Because of the well-known electronic bottleneck, direct implementation of the analog signal processors in the electronic domain would suffer from a limited operational bandwidth, slow tuning speed, poor tunability, and uneven frequency responses. Therefore, photonic processing of microwave signals has been drawing particular attentions, thanks to the intrinsic features of photonic technologies, such as a large bandwidth, low loss, light weight, wide tunability, and immunity to electromagnetic interference [1–3]. However, most previously reported systems can implement only one specific function [4–7]. When multiple functions are required, multi-stage electrical-to-optical and optical-to-electrical conversions will be required, increasing greatly the system complexity and conversion loss. Thus, a multi-function analog signal processor is attractive. Several microwave photonic systems that can implement two or more functions are reported [8–13]. In [8,9], photonic-based phase-shifted and frequency-mixed microwave signal processors are reported based on a dual-drive Mach–Zehnder modulator (DMZM). However, it is hard for the system to implement independently multi-channel phase shifting unless multiple DMZMs are employed. In addition, optical filters [8] or electrical filters [9] are employed, which may restrict the tunability of the system. In [10,11], frequency multiplying, as well as phase shifting, is implemented via a liquid crystal on a silicon-based programmable optical filter. With the programmable optical filter to select two optical sidebands and to control the amplitudes and phases, frequency-multiplied phase shifters are realized. However, the programmable optical filter is usually realized based on free-space optics, which is bulky and expensive. To avoid using an optical filter, we proposed a photonics-based analog signal processor that can realize frequency multiplying and phase shifting based on a polarization-division multiplexing dual-parallel MZM (PDM-DPMZM) [12], in which 360 deg tunable phase shifted signals with doubled or quadrupled frequency of the electrical driven signal are obtained. Although frequency multiplexing phase shifting can be regarded as a kind of frequency upconverted phase shifting, the output frequency can only be an integral multiple of the input frequency. In addition, frequency downconversion cannot be realized. Recently, a silicon-based integrated optical signal processor that can realize tens of functions is reported [13], but only a single function can be realized in one time. Once multiple functions are required, multiple processors have to be employed.

In this Letter, a photonics-based multi-function analog signal processor that can realize phase shifting, upconverting/downconverting, and filtering simultaneously or independently is proposed and demonstrated, which is indispensable in array antenna systems for signal transmitting and receiving. Since no optical filter or electrical filter is utilized, it can work over a large wavelength range and has a good frequency tunability.

Figure 1 shows the schematic diagram of the proposed multi-function photonic microwave signal processor which consists of N laser diodes (LDs), $2N$ polarization controllers (PCs), two optical combiners, a shared PDM-DPMZM, a

shared wavelength-division multiplexer (WDM), N time delay lines (TDLs), N polarizers, and a shared photodetector (PD). Each group of one LD, two PCs, one TDL, and one polarizer, together with the shared PDM-DPMZM, WDM, and PD realizes a photonic microwave frequency-mixed phase shifter. In the phase shifter, an optical carrier from the LD is directed into the PDM-DPMZM via the first PC which is inserted to align the polarization direction of the optical carrier to have an angle of 45 deg to one principal axis of the PDM-DPMZM. The PDM-DPMZM has four RF ports and six direct current (DC) biases, as shown in the dashed box of Fig. 1. Suppose the expression of the optical carrier is $\exp(j\omega_c t)$ and those of the RF signals introduced to the PDM-DPMZM are $V_{\mathrm{RF}i}\cos(\omega_{\mathrm{RF}i}t+\phi_i)$ $(i=1,2,3,4)$, where ω_c is the angular frequency of the optical carrier, $\omega_{\mathrm{RF}i}$, ϕ_i, and $V_{\mathrm{RF}i}$ are the angular frequencies, phases, and magnitudes of the four RF signals; the modulated signal after the PDM-DPMZM can be written as

$$\begin{cases} E_x = \cos(\omega_c t)\{\cos[\beta_1\cos(\omega_{\mathrm{RF1}}t+\phi_1)+\varphi_1/2]\exp(j\varphi_3) \\ \quad +\cos[\beta_2\cos(\omega_{\mathrm{RF2}}t+\phi_2)+\varphi_2/2]\} \\ E_y = \cos(\omega_c t)\{\cos[\beta_3\cos(\omega_{\mathrm{RF3}}t+\phi_3)+\varphi_4/2]\exp(j\varphi_6)' \\ \quad +\cos[\beta_4\cos(\omega_{\mathrm{RF4}}t+\phi_4)+\varphi_5/2]\} \end{cases} \tag{1}$$

where x and y represent the two principal axes of the PDM-DPMZM, $\beta_i=\pi V_{\mathrm{RF}i}/V\pi$ is the modulation index, $V\pi$ is the half-wave voltage, $\varphi_m=\pi V_{\mathrm{DCm}}/V\pi$ $(m=1,2,3,4,5,6)$ are the phase differences introduced by the DC biases, and V_{DCm} are the voltages of the DC biases. Controlling the DC biases to let $\varphi_1=\varphi_2=\varphi_4=\varphi_5=\pi$, $\varphi_3=\varphi_6=\pi/2$ and letting the parameters of the signals satisfy $V_{\mathrm{RF2}}=V_{\mathrm{RF1}}$, $\omega_{\mathrm{RF2}=}\omega_{\mathrm{RF1}}$, $V_{\mathrm{RF4}}=V_{\mathrm{RF3}}$, $\omega_{\mathrm{RF4}=}\omega_{\mathrm{RF3}}$, $\phi_2=\phi_1+\pi/2$, $\phi_4=\phi_3+\pi/2$, and $\phi_1=\phi_3=0$, Eq. (1) can be rewritten as

$$\begin{cases} E_x = -2J_{\pm1}(\beta_1)\exp[j(\omega_c t\pm\omega_{\mathrm{RF1}}t\pm\pi/2)] \\ E_y = -2J_{\pm1}(\beta_3)\exp[j(\omega_c t\pm\omega_{\mathrm{RF3}}t\pm\pi/2)] \end{cases}. \tag{2}$$

where J_p is the Bessel Function of the first kind of order p. In writing Eq. (2), small-signal modulation is assumed so that higher-order (≥ 2) sidebands are ignored. As can be seen from Eq. (2), each polarization direction contains only one sideband, indicating that carrier-suppressed single-sideband (CS-SSB) modulation is successfully realized along each polarization direction. The two CS-SSB modulated signal contains the same sideband, i.e., the upper +1st-order or the lower −1st-order sideband. Therefore, two orthogonally polarized wavelengths that are separated by the difference of the frequencies of the two original RF signals are obtained. When we combine the two orthogonally polarized wavelengths with a polarizer that has an angle of α

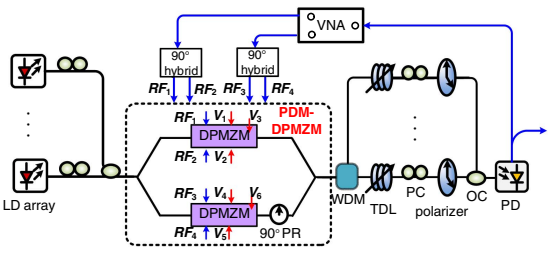

Fig. 1. Schematic diagram of the proposed multi-function analog signal processor. VNA, vector network analyzer.

to one principal axis of the PDM-DPMZM and lead the signal after the polarizer to the PD for square-law detection, an electrical current is obtained:

$$I_{\mathrm{AC}}(t)\propto J_{\pm1}(\beta_1)J_{\pm1}(\beta_3)\cos\alpha\sin\alpha\cos(\omega_{\mathrm{RF3}}t-\omega_{\mathrm{RF1}}t). \tag{3}$$

An RF signal with a frequency that is the difference of the frequencies of the two driven signals is generated, i.e., down-conversion is realized. On the other hand, when two DC biases are controlled to let $\varphi_3=-\varphi_6=\pm\pi/2$, the signals after the polarizer and PD are written as

$$I_{\mathrm{AC}}(t)\propto J_{\pm1}(\beta_1)J_{\mp1}(\beta_3)\cos\alpha\sin\alpha \times\cos(\omega_{\mathrm{RF3}}t+\omega_{\mathrm{RF1}}t), \tag{4}$$

so an RF signal with a frequency that is the sum of the frequencies of the two driven signals is generated, i.e., upconversion is implemented.

If a PC is inserted before the polarizer to rotate the two orthogonally polarized wavelengths in Eq. (2) by 45 deg and add a phase difference of 90 deg [14], the current in Eq. (4) becomes

$$I_{\mathrm{AC}}(t)\propto 2J_{\pm1}(\beta_1)J_{\pm1}(\beta_3)\cos(\omega_{\mathrm{RF3}}t-\omega_{\mathrm{RF1}}t-2\alpha). \tag{5}$$

As can be seen from Eq. (5), the phase of the generated down-converted signal can be continuously tuned by simply controlling the polarization angle α while keeping the magnitude unchanged. It should be noted that the magnitude-invariability can only be present when the polarization extinction ratio of the modulator is large (>30 dB for instance). Similarly, if the signal in Eq. (4) is rotated by a PC and combined by a polarizer, the current after PD can be expressed by

$$I_{\mathrm{AC}}(t)\propto 2J_{\pm1}(\beta_1)J_{\mp1}(\beta_3)\cos(\omega_{\mathrm{RF3}}t+\omega_{\mathrm{RF1}}t-2\alpha). \tag{6}$$

As a result, a microwave photonic frequency-mixed phase shifter is realized. Multi-channel phase shifting can be realized in the system with a shared laser source and PDM-DPMZM, since the phase of the frequency-mixed signal can be split into a number of branches and independently adjusted by a PC in each branch [12]. It should also be noted that, if one of ω_{RF1} and ω_{RF3} equals 0, the photonic phase-shifted mixer is equivalent to a photonic microwave phase shifter [15]. The phase shifter can be tuned in a very fast speed [16], and can be employed to generate frequency-mixed and phase-coded signals [14,16,17]. Based on the photonic microwave frequency-mixed phase shifter, an N-tap MPF with all complex coefficients can be built. The transfer function of the MPF is given by [18]

$$H(f)=\sum_{q=0}^{N-1}a_q\exp(j\theta_0)\exp\left[jq2\pi T\left(\frac{\theta}{2\pi T}-f\right)\right], \tag{7}$$

where $a_q\exp(j\theta_0)$ is the tap coefficient of the MPF, θ_0 is the phase shift of the first tap, T is the unit delay of the filter which is introduced by the TDL, and θ is the phase difference between the adjacent taps. The center frequency of the MPF is $\theta/2\pi T$, which can be continuously tuned by the phase difference θ. In practice, $\theta/2\pi T$ should be set to $(\omega_{\mathrm{RF3}}\pm\omega_{\mathrm{RF1}})/2\pi$ to pass the mixed signal and remove the mixing spurs.

To demonstrate the feasibility of the proposed multi-function photonic microwave signal processor, an experiment is carried out based on the setup shown in Fig. 1. A four-channel tunable laser source (TLS, Agilent N7714A) is employed as the laser

array to implement a four-channel photonics-based analog signal processor. Four lightwaves separated by 1.6 nm (corresponding to 200 GHz) with powers of 13 dBm are generated by the TLS and sent to a PDM-DPMZM (Fujitsu FTM 7977HQA) with a 3 dB bandwidth of 23 GHz and a half-wave voltage of 3.5 V. The polarization extinction ratio of PDM-DPMZM is 22 dB. The modulator is driven by four RF signals obtained by splitting two RF signals from a four-port vector network analyzer (VNA, R&S ZVA67) with two 90 deg hybrids (1.7–36 GHz). By carefully adjusting the DC biases of the modulator, orthogonally polarized CS-SSB modulated signals at the four wavelengths are generated by the PDM-DPMZM, which are then split into four paths with a four-channel WDM. In each path, a TDL is followed to adjust the time delay, and a PC is inserted to adjust the angle between the polarization direction of the polarizer and the principal axis of the PDM-DPMZM. Then the four wavelengths are combined by an optical combiner. A PD with a bandwidth of 40 GHz and a responsivity of 0.65A/W is used to perform optical-to-electrical conversion. The optical spectra are measured by an optical spectrum analyzer (OSA, AQ6370C), the electrical spectra are measured by an electrical spectrum analyzer (ESA, R&S FSV40), and the frequency responses are measured by the VNA.

First, only one channel (1549.32 nm) is connected to realize the photonic microwave frequency-mixed phase shifter. Figure 2 shows the optical spectra at the output of the PDM-DPMZM. To realize CS-SSB modulations, the two sub-DPMZMs of the PDM-DPMZM are driven by two pairs of orthogonal RF signals which are obtained by splitting two RF signals with two 90 deg hybrids. The frequencies of the two RF signals are set to be 10 and 5 GHz. The output optical spectra of the PDM-DPMZM are shown in Figs. 2(a) and 2(b). Figure 2(a) illustrates two +1st-order sidebands separated by the difference of the frequencies of the two RF driven signals, while Fig. 2(b) shows a −1 st-order sideband (10 GHz) and a +1 st-order sideband (5 GHz) that separated by the sum frequency of the two RF signals. In both conditions, the optical carrier and second-order sidebands are effectively suppressed. According to [19], the third-order intermodulation distortion is also significantly reduced, as it originates mainly from the product of the fundamental and the second-order components, and the product of the optical carrier and the third-order components.

To confirm the polarization orthogonality of the two optical sidebands, a PBS is connected. The two outputs of the PBS are shown as the black dotted line (10 GHz) and red dashed line (5 GHz). As can be seen, CS-SSB modulations are successfully implemented along the two polarization directions. The polarization extinction ratio is about 30 dB for upconversion and about 20 dB for downconversion. The relatively low polarization extinction ratio for the downconversion case is mainly due to the limited resolution of the OSA (0.02 nm).

To evaluate the tunability of the proposed system, one RF signal adjusted from 2 (or 12) to 20 GHz and another frequency-fixed RF signal at 10 GHz are used to drive the two sub-DPMZMs. The optical spectra of the downconverted signals are shown in Fig. 3(a), while those of the upconverted signals are depicted in Fig. 3(b). As can be seen, for all frequencies, only two strong sidebands are presented.

To observe the phase response of the system, one RF signal is replaced by a frequency-swept signal, while the other is still fixed at 10 GHz. For downconversion, the signal is swept from 10 to 23 GHz, while for the upconversion, the frequency is swept from 0 to 23 GHz. By adjusting the PC before the polarizer, which changes the angle between the polarization direction of the polarizer and the principal axis of the PDM-DPMZM, the phase of the generated RF signal is continuously tuned from −180 to 180 deg, as shown in Figs. 4(a) and 4(b). Flat phases over the full range of the difference frequency (0–13 GHz) and the sum frequency (10–33 GHz) are observed, indicating that a frequency-mixed phase shifter is realized.

Then all four channels are connected, and the wavelengths of the four optical carriers are 1547.72, 1549.32, 1550.92, and 1552.52 nm. Figure 5 shows the measured frequency responses of the four-tap MPF. The frequency responses of the four-tap MPF around 5.5 and 11.5 GHz are shown in Figs. 5(a) and 5(b), respectively, which are observed under a downconversion condition. The free spectra range (FSR) is about 170 MHz, corresponding to a unit time of 5.88 ns. The mainlobe-to-sidelobe suppression ratio is about 14 dB. By adjusting the PCs in the four taps to introduce different phase shifts, the center frequency of the MPF can be continuously tuned over the full FSR range without changing the shape of the frequency

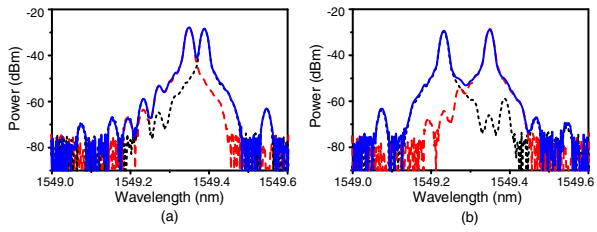

Fig. 2. Optical spectra at the output of the PDM-DPMZM when two RF signals with frequencies of 10 and 5 GHz are applied to the two DPMZMs, respectively. (a) Downconversion and (b) upconversion.

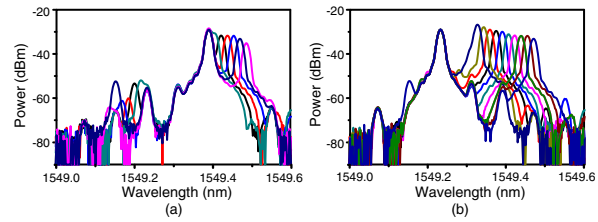

Fig. 3. Optical spectra at the output of the PDM-DPMZM for (a) downconversion with one input tuned from 12 to 20 GHz and the other fixed at 10 GHz, and (b) upconversion with one input tuned from 2 to 20 GHz and the other fixed at 10 GHz.

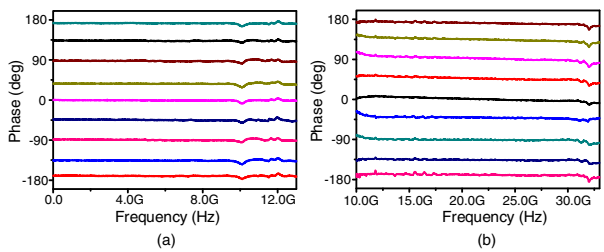

Fig. 4. Phase responses of the phase shifter with (a) downconversion and (b) upconversion.

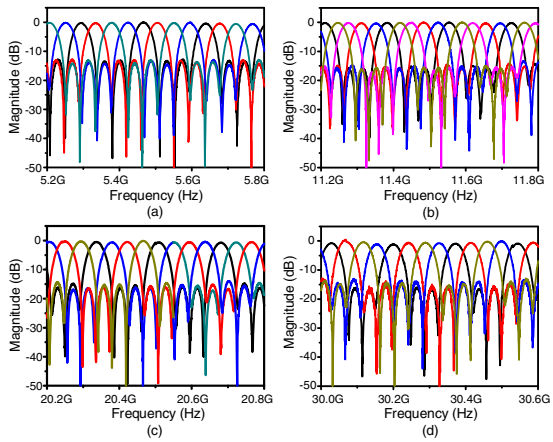

Fig. 5. Frequency responses of the four-tap MPF with different center frequencies (a) and (b) under the downconversion condition, and (c) and (d) under the upconversion condition.

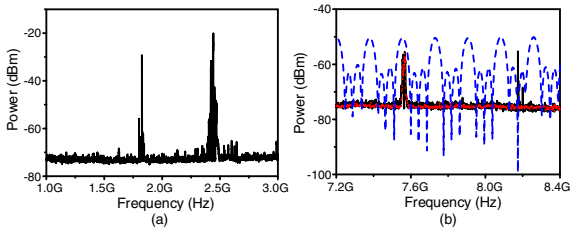

Fig. 6. (a) Electrical spectra of the received signal of a WiFi antenna and (b) the electrical signal with (dotted) or without (solid) the MPF and the transmission frequency response of the MPF (dashed).

response. Similarly, the frequency responses under an upconversion condition are shown in Figs. 5(c) and 5(d), which are around 20.5 and 30.5 GHz, respectively. The FSR are the same as that under the downconversion condition, and the center frequency can also be continuously tuned.

To investigate the feasibility of the proposed photonics-based analog signal processer in real applications, one of the RF signals is achieved from a WiFi antenna, while the other signal is still fixed at 10 GHz. Figure 6(a) shows the electrical spectra of the received signal from the WiFi antenna. Relatively strong 1.8 and 2.4 GHz components, corresponding to a two-generation (2G) mobile communication signal and WiFi signal, are clearly observed. We assume a scenario in which only the WiFi signal is required to be upconverted, while the 2G signal is undesired. First, only one tap of the proposed analog signal processor is connected, with the generated signal shown as the black line in Fig. 6(b). Signals with frequencies around 7.6 and 8.2 GHz are observed, showing that the two signals are upconverted to the high-frequency band. Then all the four taps are connected. The frequency response of the system is shown as the blue line in Fig. 6(b), which contains a passband around 7.6 GHz and a stop band over 8.2 GHz. The signal after filtering is illustrated as the red line of Fig. 6(b), from which we can see that only the signal around 7.6 GHz is left, and the signal around 8.2 GHz is removed by the MPF.

In conclusion, a novel photonics-based multi-function analog signal processor, which can implement simultaneously phase shifting, upconversion/downconversion, and filtering, was proposed and demonstrated based on a PDM-DPMZM. With only one tap connected, a phase shifter with the phase continuously tuned from −180 to 180 deg was realized. The frequency of the signal after the processor can be the sum or difference frequency of the two input RF signals. With all the taps connected, a four-tap MPF was implemented. The filtered signal is the frequency upconverted/downconverted signal, and its phase is determined by the setting of the MPF taps. The frequency response can be tuned over the full FSR range while maintaining the shape unchanged. The proposed system is extremely flexible, which can find applications in beamforming networks, RF frontends, and radio over fiber systems.

Funding. National Natural Science Foundation of China (NSFC) (61422108, 61527820); Funding for Outstanding Doctoral Dissertation in NUAA (BCXJ15-02); Funding of Jiangsu Innovation Program for Graduate Education (KYLX15_0280).

REFERENCES

1. J. Capmany, B. Ortega, and D. Pastor, J. Lightwave Technol. **24**, 201 (2006).
2. J. P. Yao, J. Lightwave Technol. **27**, 314 (2009).
3. S. L. Pan, D. Zhu, S. F. Liu, K. Xu, Y. T. Dai, T. L. Wang, J. G. Liu, N. H. Zhu, Y. Xue, and N. J. Liu, IEEE Microw. Mag. **16**(8), 61 (2015).
4. D. Pastor, J. Capmany, and B. Ortega, IEEE Photon. Technol. Lett. **12**, 77 (2000).
5. Z. Z. Tang and S. L. Pan, IEEE Microw. Wireless Compon. Lett. **26**, 67 (2016).
6. A. Byrnes, R. Pant, E. Li, D. Y. Choi, C. G. Poulton, S. H. Fan, S. Madden, B. L. Davies, and B. J. Eggleton, Opt. Express **20**, 18836 (2012).
7. W. Li, M. Li, and J. P. Yao, IEEE Trans. Microwave Theory Tech. **60**, 1287 (2012).
8. Z. Z. Tang and S. L. Pan, J. Lightwave Technol. **34**, 4729 (2016).
9. T. Jiang, R. Wu, S. Yu, D. Wang, and W. Gu, Opt. Express **25**, 4519 (2017).
10. Z. H. Feng, S. N. Fu, T. Ming, and D. M. Liu, IEEE Photon. J. **6**, 5500108 (2014).
11. H. Z. Li, T. Y. Huang, C. J. Ke, S. N. Fu, P. P. Shum, and D. M. Liu, IEEE Photon. Technol. Lett. **26**, 220 (2014).
12. Y. M. Zhang and S. L. Pan, Opt. Lett. **41**, 1261 (2016).
13. D. Perez, I. Gasulla, L. Crudgington, D. J. Thomson, A. Z. Khokhar, K. Li, W. Cao, G. Z. Mashanovich, and J. Capmany, Nat. Commun. **8**, 636 (2017).
14. Y. M. Zhang, F. Z. Zhang, and S. L. Pan, IEEE Trans. Microw. Theory Tech. **65**, 651 (2017).
15. S. L. Pan and Y. M. Zhang, Opt. Lett. **37**, 4483 (2012).
16. Y. M. Zhang and S. L. Pan, Opt. Lett. **38**, 766 (2013).
17. Y. M. Zhang, X. W. Ye, Q. S. Guo, F. Z. Zhang, and S. L. Pan, J. Lightwave Technol. **35**, 1821 (2017).
18. Y. M. Zhang and S. L. Pan, Opt. Lett. **38**, 802 (2013).
19. S. Y. Li, X. P. Zheng, H. Y. Zhang, and B. K. Zhou, IEEE Photon. Technol. Lett. **22**, 1775 (2010).

157.0.76.109 {ts '2017-12-05 06:31:29'}